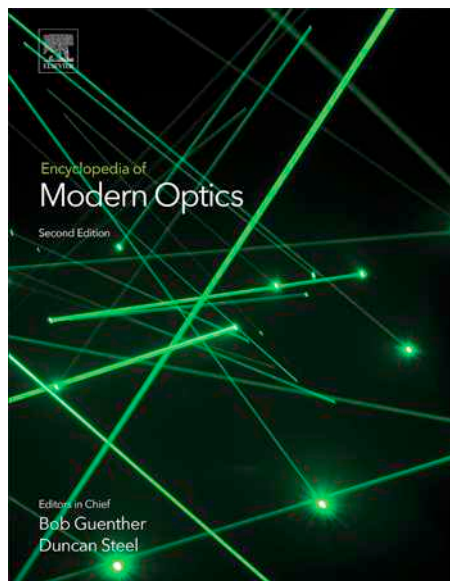


**Provided for non-commercial research and educational use.
Not for reproduction, distribution or commercial use.**

This article was originally published in the *Encyclopedia of Modern Optics 2nd edition*, published by Elsevier, and the attached copy is provided by Elsevier for the author's benefit and for the benefit of the author's institution, for non-commercial research and educational use including without limitation use in instruction at your institution, sending it to specific colleagues who you know, and providing a copy to your institution's administrator.



All other uses, reproduction and distribution, including without limitation commercial reprints, selling or licensing copies or access, or posting on open internet sites, your personal or institution's website or repository, are prohibited. For exceptions, permission may be sought for such use through Elsevier's permissions site at:

<http://www.elsevier.com/locate/permissionusematerial>

Karthik Vishwanath, Sara Zanfardino (2018) In Situ Optical Tissue Diagnostics/Laser Speckle-Based Spectroscopy Techniques in Biomedicine. In: Guenther, R. and Steel, D. (eds.), *Encyclopedia of Modern Optics 2nd edition*, vol. 3, pp. 95–99. Oxford: Elsevier.

© 2018 Elsevier Ltd. All rights reserved.

In Situ Optical Tissue Diagnostics/Laser Speckle-Based Spectroscopy Techniques in Biomedicine

Karthik Vishwanath and Sara Zanfardino, Miami University, Oxford, OH, United States

© 2018 Elsevier Ltd. All rights reserved.

Nomenclature

\vec{r} Vector location of a point of interest in space
 τ Correlation time
 $\Phi(\vec{r})$ Photon fluence rate
 μ_a Absorption coefficient of medium

μ_s Scattering coefficient of medium
 D Optical diffusion coefficient of medium
 $S(\vec{r})$ Input source term
 g Anisotropy coefficient for single scattering of medium

Glossary

Absorption coefficient A wavelength-dependent medium property characterizing the probability of photon absorption in the medium.

Anisotropy coefficient A wavelength-dependent medium property characterizing the mean cosine of the angle between the directions of photon incidence and scattering in the medium.

Coherence The correlation between two (electromagnetic) waves either at different points in space (spatial coherence) or at two different points in time (temporal coherence).

Photon fluence rate The number of photons passing through a specified area per unit of time.

Photon radiance The net photon power passing through a specified area, along a specified direction, per unit of time.

Scattering coefficient A wavelength-dependent medium property characterizing the probability of photon scattering in the medium.

Speckle Small “spots” of bright and dark spots formed when a coherent source is incident on any surface due to constructive and destructive interference at the detector plane.

Temporal autocorrelation function The correlation of a time-dependent function, with itself across the full time-period measured of the original function.

Turbid medium Any medium appears “cloudy” or “murky” due multiple light scattering.

Introduction

Optical spectroscopic methods and techniques have been used for sensing of turbid media such as biological tissues and is an active area of research in the biomedical sciences. The basic prescription in most applications of these methods is to non-invasively derive optical properties of media using experimental measurements in combination with mathematical modeling and analysis to yield quantitative analogues of physiological markers related to human health and disease. Clinical applications over the last two decades have reported using optical spectroscopy for several applications including detection (including surgical margin identifications) of cancer, detection of atherosclerotic plaques, monitoring of burns, wounds and their healing, measuring cerebral functions, and imaging of retinal and dental health.

Optical techniques used for biosensing may be classified as two broad categories – static or dynamic – depending on whether the experimental techniques and methods used are inherently time-integrated, or time-resolved. A large fraction of optical methods that are used to characterize tissue optical properties including diffuse optical spectroscopy and tomography fall under the realm of static techniques – wherein one or more light sources are used to illuminate a medium of interest and a set of measurements (usually at several spatial locations) which are translated to produce a static spatial map of optical properties. It is to be noted that repeated measurements of such static optical techniques as defined here may still be used to study tissue (or biological) dynamics, at time-scales of the acquisition rates of the measurements. Dynamic optical spectroscopic techniques on the other hand make a set of measurements (again at one or more spatial locations) by measuring changes or fluctuations in light intensities (or a shift in the frequency spectrum) across several decades in time and seek to relate these fluctuations to a dynamical varying physical quantity such as motion of particles in the medium.

This article describes a dynamic optical technique – diffuse correlation spectroscopy (DCS) – which combines the theoretical formalism of incoherent photon propagation in a strongly scattering medium, to model experimental measurements of dynamic speckle intensity fluctuations (correlations) measured from the same medium. In DCS, measured speckle intensity fluctuations from an incident monochromatic source is used to compute temporal intensity autocorrelations which in turn are used to extract information about movement of scatterers within the volume of tissue probed by the diffuse optical waves transporting the incident light field to the detector. A closely related optical technique to DCS is Laser Doppler flowmetry which detects the scattered, frequency-shifted spectrum of a monochromatic (coherent) light source after passing through a scattering medium containing moving scatterers. Although these two techniques are closely connected analytically and theoretically as Fourier

transforms of each other, their experimental implementations and analysis are quite distinct. This article will only focus on the description, analysis and applications of DCS for tissue sensing.

Historical Overview and Background

When coherent light is scattered by a material, temporal measurements of the scattered field intensity exhibits fluctuations. Theoretical calculations of such fluctuations of light intensity when scattered by molecules (or other particles) have been studied since beginning of 20th century and include contributions from Einstein, Raleigh, Smoluchowski, and Debye. With the invention of the laser and fast detector-electronics, dynamic light scattering (DLS) became an accessible experimental technique to measure and study a wide variety of dynamic phenomena in complex media such as molecular rotation or diffusion in complex fluids, colloidal particle compositions and biological systems. Historically, DLS theory was developed first for weakly scattering systems (single scattering limit). However, experimentally, the methods of DLS are as applicable to multiply scattering systems as they were to weakly scattering media. DLS was soon applied to study of particle dynamics in various multiply scattering materials and the theoretical modeling of such experimental measurements came to be called diffusing wave spectroscopy (DWS). Experimentally, DCS uses the same experimental theme that is employed in DLS (or DWS) – but instead provides an elegant theoretical encapsulation to analyze the experimental measurements using the now well-established framework of diffusive optical transport in turbid media as sketched in Fig. 1.

Experimentally, all of these techniques employ a long-coherence length laser to illuminate the sample of interest and collect the scattered light intensity from a small volume. Fluctuations in the measured intensity incident on a photodetector and photon-counting system, $I(\vec{r}, t)$ can be obtained. The experimentally calculated intensity unnormalized and normalized correlation functions of these fluctuations are denoted respectively using their standard notations as:

$$G_2(\vec{r}, \tau) = \langle I(\vec{r}, 0) \cdot I(\vec{r}, \tau) \rangle = \lim_{T \rightarrow \infty} \frac{1}{T} \int_0^T I(\vec{r}, t) I(\vec{r}, t + \tau) dt \quad (1)$$

$$g_2(\vec{r}, \tau) = \frac{\langle I(\vec{r}, 0) \cdot I(\vec{r}, \tau) \rangle}{\langle I(\vec{r}, 0) \rangle^2} \quad (2)$$

The integral in Eq. (1) defines the temporal correlation function of $G_2(r, \tau)$ for an infinitely long time-signal $I(\vec{r}, t)$ while the angular brackets indicate ensemble averages. Although it is usually assumed that the system under observation is ergodic and thus ensemble averages are time averages this may not always be true – we discuss this in the section under Experimental Considerations below. In practice, the temporal correlation is usually calculated using a correlator board (or computer) to numerically evaluate the integral in Eq. (1). The smaller dt is, the more accurately measurements can be expected to match theoretical predictions, with the longest possible correlation time being the total duration of continuous data acquisition. Photodetectors with sampling rates in the 10–100 MHz range are typically used to collect DCS data for 1–10 s for in vivo tissue sensing.

Theoretically, the (detected) intensity is related to the scattered complex electric field from a monochromatic coherent source as $I(\vec{r}, t) = E(\vec{r}, t)E^*(\vec{r}, t) = |E(\vec{r}, t)|^2$ and the corresponding correlations of the detected unnormalized and normalized electric fields are defined as per convention by:

$$G_1(\vec{r}, \tau) = \langle E(\vec{r}, 0)E^*(\vec{r}, \tau) \rangle \quad (3)$$

$$g_1(\vec{r}, \tau) = \frac{\langle E(\vec{r}, 0)E^*(\vec{r}, \tau) \rangle}{\langle E(\vec{r}, 0) \rangle} \quad (4)$$

From the above definitions some properties of the field correlation functions can be computed. $G_1(\vec{r}, 0) = \langle |E(\vec{r}, t)|^2 \rangle = \langle I(\vec{r}, 0) \rangle$, giving $g_1(\vec{r}, 0) = 1$. Also, for long correlation times $G_1(\vec{r}, \tau) = \langle E(\vec{r}, t) \rangle^2 = 0$, giving $g_1(\vec{r}, \tau) = 0$. Given that it is the field fluctuations that give rise to the measured intensity fluctuations, theoretical methods are

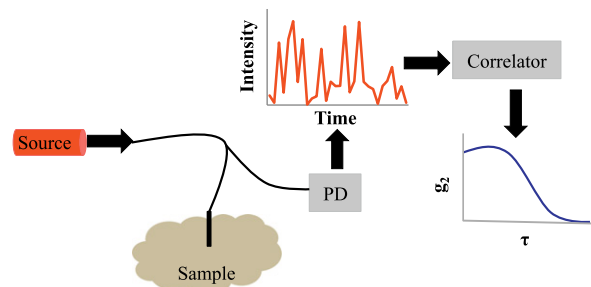


Fig. 1 Schematic representation of the DCS setup and its components. The illumination is provided by a laser source coupled to the sample using fiber optical probes. The detected signal is measured using a photodetector (PD) that can provide continuous (temporal) measurements. The monitored intensity fluctuations are recorded using a correlator device to compute the normalized intensity correlation g_2 .

used to generate models that predict behavior of $G_1(\vec{r}, \tau)$ and $g_1(\vec{r}, \tau)$. If the temporal fluctuations in $E(\vec{r}, t)$ are random and assumed to arise due to uncorrelated motions of several randomly (diffusing or moving) particles, then these fluctuations in $E(\vec{r}, t)$ will be normally distributed. Under this condition, $G_1(\vec{r}, \tau)$ and $G_2(\vec{r}, \tau)$ (and their normalized counterparts) are theoretically related through the Siegert relations:

$$G_2(\vec{r}, \tau) = \langle I(\vec{r}, 0) \rangle^2 + |G_1(\vec{r}, \tau)|^2 \quad (5)$$

$$g_2(\vec{r}, \tau) = 1 + |g_1(\vec{r}, \tau)|^2 \quad (6)$$

In DCS the functional form for $G_1(\vec{r}, \tau)$ is hypothesized to follow the same diffusion transport equation governing photon propagation in a multiply scattering medium, while $g_1(\vec{r}, \tau)$ is modeled using the random, independent single scattering model using the formalism of DLS.

Diffusive Photon Correlation Transport

Photon propagation in a turbid medium can be accurately modeled as a random walk of neutral particles in the medium using optical transport coefficients of the medium – typically specified as absorption, scattering and anisotropy. The radiative transport equation provides a theoretical analog for describing propagation of photon radiance within such media. The mathematical form of the transport equation prevents its use practice since it remains intractable for appropriately modeling experimental (boundary) conditions. The transport equation however reduces to a diffusion type equation if two conditions are met (a) if the medium's absorption is small in comparison to its scattering and (b) if the detected light has been scattered sufficiently and can be thus be considered emanating from an isotropic source. Both these conditions can largely experimentally satisfied – the first by selecting light with appropriate wavelengths, since the absorption and scattering properties of tissue are strongly wavelength dependent (for e.g. the near-infrared (NIR) wavelengths for tissue spectroscopy). The second condition may be satisfied by keeping the source-detector separations large in comparison to the mean scattering transport length of light in the medium of interest.

Under steady-state conditions (i.e. the source is CW or when the detected signal is time-integrated for longer than a few ns, in general) the diffusion equation for a semi-infinite homogenous medium with uniform optical properties the diffusion equation is written as:

$$[D\nabla^2 - \mu_a]\Phi(\vec{r}) = S(\vec{r}) \quad (7)$$

Here, $\Phi(\vec{r})$ represents the photon fluence rate (Wm^{-2}) as the net light energy at all points of interest in the medium, $S(\vec{r})$ describes the input source term, and D the medium's diffusion coefficient given by $D = 3[\mu_a + \mu_s(1 - g)]$, where μ_a is the medium's absorption coefficient, μ_s its scattering coefficient and g the single-scattering anisotropy coefficient. Under the formalism of DCS, the unnormalized field correlation $G_1(\vec{r}, \tau)$ is propagated using the diffusion equation as:

$$\left[D\nabla^2 - \mu_a - \frac{1}{3}\mu_s(1 - g)k_0^2 \langle \Delta r^2(\tau) \rangle \right] G_1(\vec{r}, \tau) = S(\vec{r}) \quad (8)$$

The $\langle \Delta r^2(\tau) \rangle$ in Eq. (8) is the only additional term for the transport of the field correlation in a homogenous turbid medium and represents the mean-square displacement of the diffusing (or moving) particles, which add to the dynamics of the decay in the field correlation. Since closed form expressions of $\Phi(\vec{r})$ for Eq. (7) are readily available for several geometries, they can be used to calculate $G_1(\vec{r}, \tau)$ for measurements made in those geometries by replacing μ_a with $\mu_a - \frac{1}{3}\mu_s(1 - g)k_0^2 \langle \Delta r^2(\tau) \rangle$.

Experimental Considerations

Experimentally, one has to make choices about the illuminating source, the delivery and collection optics to couple to the medium, and the detection system (see Fig. 1). Fig. 2 shows representative examples of experimental measurements obtained using a fiber-based DCS system while for different light sources, different detection fiber sizes and different types of scattering media.

Light Sources

Given that the theoretical formulation for modeling measurements assumes a monochromatic plane wave, DCS sources are usually single mode, stabilized, long-coherence length lasers operating in between 600–800 nm. In order for the experimental data to contain reliable dynamic information about the motion of scatterers, the temporal coherence length must be much longer the average path length of photons diffusing from the source and the detector placed on the tissue. Most applications reported with DCS use sources with coherence lengths longer than several meters.

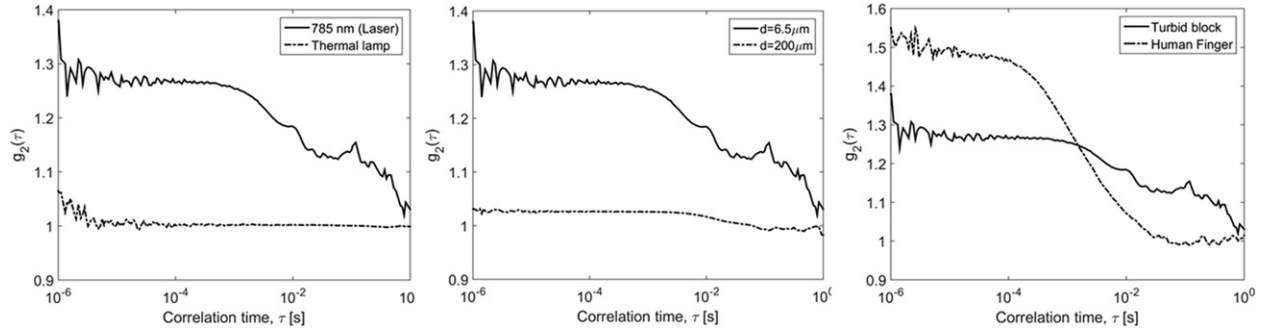


Fig. 2 Measured representative intensity correlation curves (g_2) depicting data obtained for changing incident light source (left), changing detection fiber radius (middle) and different media (right). In all the plots, the solid line represents the autocorrelation detected using a fiber probe (source fiber radius = 200 μm , detector fiber radius = 6.5 μm and center-center distance of 1.5 mm) in reflection geometry on a turbid solid block. The dashed line in the left shows the correlation when the source was changed to a thermal halogen lamp. In the middle figure, the second fiber probe was used that had identical properties as the first probe but with detector radius of 200 μm while using the laser light for illumination. The dashed line in the right figure shows data from the first probe in contact with a human finger under laser illumination. These data indicate how both the intercept on the y-axis as well as the decay curves change across different conditions.

Coupling Optics

Although it is possible to make DCS devices capable of operating in a non-contact mode (i.e. coupling light to and from the medium without physical contact), the most practical method of using DCS for biomedical applications has been to couple light from the source to a medium (tissue site) using a source-fiber and obtaining diffusely scattered measurements using one or more detection fibers. The detection fiber is typically a low-mode fiber (ideally capable of monitoring fluctuations of a single speckle) while the source-fiber is a multi-mode fiber. The common end of this probe sets the source-detector geometry used to probe the sample volume and usually is larger than 5–10 mm for most DCS systems to stay within validity limits of diffusion theory.

Detection Systems

The ability to extract temporal correlations relies which not only requires sampling a fluctuating intensity signal at sampling rates of 10–100 MHz but also to store and process these signals to obtain the required intensity autocorrelation function. Traditional photon detection systems used an amplified photomultiplier tube (PMT) that with high enough response rates, while most recent systems employ detectors are small-area single photon avalanche photodiodes (APD). The digitized output sampled off the photodetector is to a digital correlator – usually a dedicated hardware board that computes required time correlation functions.

Modeling Measured Intensity Correlations

As described above, the experimental observations yield $g_2(\vec{r}, \tau)$ that is the intensity correlation for a measured at the detector situated at location \vec{r} relative to the source and the medium. Thus, the analytical expressions for $G_1(\vec{r}, \tau)$ are converted to calculate $g_1(\vec{r}, \tau)$ which in turn is related to the experimental measurement of $g_2(\vec{r}, \tau)$ as:

$$g_2(\vec{r}, \tau) = 1 + \beta |g_1(\vec{r}, \tau)|^2 \quad (9)$$

Here, β is an experimental factor that is lesser than unity and depends on specific experimental configuration details such as the coherence length, coupled modes, dark noise and detection aperture size and thus is usually obtained as a free parameter during the fitting process. Besides β , experimentally measured data is fit to a specified functional formulation to extract parameters contributing to $\langle \Delta r^2(\tau) \rangle$. For example two commonly used models in tissue spectroscopy include diffusive flow where $\langle \Delta r^2(\tau) \rangle = 6D_B\tau$ where D_B is a diffusion coefficient, or random flow where $\langle \Delta r^2(\tau) \rangle = V^2\tau^2$ and V^2 is the second moment of the moving particle's velocity distribution. It is important to note that analytical fitting process is possible only by having estimates for the optical absorption and scattering coefficients of the medium, at the wavelength of the incident source.

Applications to In Vivo Tissue Sensing

Fiber-based DCS measurements have been obtained across a variety of clinical settings to address problems in monitoring progress of treatments, for monitoring cerebral blood flow during ischemia and for assessment of wound healing. Ultimately, the largest factor of contrast in biological tissues for the decorrelation of the measured intensity autocorrelations is attributed to the motion

of red blood cells in the vascular system. Thus, nearly any health application that requires monitoring of blood flow and its relative changes across perturbations could potentially use DCS a simple, non-invasive clinical adjunct.

DCS has been explored to investigate tissue perfusion since angiogenesis (i.e. the growth of new blood vessels) is now believed to be a marker of tumor growth and progression. Further, since treatments of tumors including chemotherapy and photodynamic therapy would be expected to impact blood flow and its dynamics during such treatments, DCS measurements have been applied to investigate these changes longitudinally in cancers of the prostate, breast and of the head and neck. In many cases DCS has been shown to provide an early indicator of treatment response (and failure). Given that traditional therapy monitoring techniques that include methods such as PET, MRI or CT, which many times are not accessible or amenable for use, DCS may provide a convenient, clinically-adoptable alternative.

DCS has also been used in applications to monitor cerebral blood flow – such monitoring studies were focused particularly on investigating perfusion rates and changes in the brain during ischemic strokes. An ischemic stroke the most common type of hemorrhagic stroke where a blood clot in the body constricts or depletes blood supply to certain regions of the brain. Since such a blockage would result in markedly different perfusion rates, DCS was an appropriate candidate for continuous and non-invasive blood in patients.

Other clinical applications of DCS have explored monitoring patient recovery from a traumatic wound injury, monitoring the blood supply to maxillofacial autographs during early stages of transplant, and monitoring the blood supply to skeletal tissues and muscles during certain high-intensity activities such as exercise. Several of these studies that employ DCS for measurement of tissue perfusion have been validated against clinically used “gold-standards” for flow-monitoring such as CT and MRI.

Preliminary and current data in clinical trials is promising for the field of non-invasive biomedical optical sensing. With an increasing number of studies showing successful applications of dynamic light scattering spectroscopy for in vivo and real-time monitoring of blood flow in tissues, it is likely that DCS-based devices will become more widespread. These application areas will benefit if DCS devices become commercially available as out-of-the box instruments and could become a routine and important tool used for sensing in vascular function or dysfunction in humans.

Further Reading

- Ackerson, B.J., Dougherty, R.L., Reguigui, N.M., Nobbmann, U., 1992. Correlation transfer – Application of radiative-transfer solution methods to photon-correlation problems. *Journal of Thermophysics and Heat Transfer* 6, 577–588.
- Berne, B.J., Pecora, R., 1990. In *dynamic light scattering with applications to chemistry*. New York: Wiley-Interscience.
- Boas, D.A., Yodh, A.G., 1997. Spatially varying dynamical properties of turbid media probed with diffusing temporal light correlation. *Journal of the Optical Society of America* 14, 192–215.
- Bonner, R., Nossal, R., 1981. Model for laser Doppler measurements of blood flow in tissue. *Applied Optics* 20, 2097–2107.
- Briers, J.D., 2001. Laser Doppler, speckle and related techniques for blood perfusion mapping and imaging. *Physiological Measurement* 22, R35–R66.
- Durduran, T., Choe, R., Baker, W.B., Yodh, A.G., 2010. Diffuse optics for tissue monitoring and tomography. *Reports on Progress in Physics* 73 (7), doi:10.1088/0034-4885/73/7/076701.
- Farzam, P., Zirak, P., Binzoni, T., Durduran, T., 2013. Pulsatile and steady-state hemodynamics of the human patella bone by diffuse optical spectroscopy. *Physiological Measurement* 34, 839–857.
- Kim, M.N., Durduran, T., Frangos, S., *et al.*, 2010. Noninvasive measurement of cerebral blood flow and blood oxygenation using near-infrared and diffuse correlation spectroscopies in critically brain-injured adults. *Neurocritical Care* 12, 173–180.
- Pine, D.J., Weitz, D.A., Chaikin, P.M., Herbolzheimer, E., 1988. Diffusing wave spectroscopy. *Physical Review Letters* 60, 1134–1137.
- Yu, G., 2012. Near-infrared diffuse correlation spectroscopy in cancer diagnosis and therapy monitoring. *Journal of Biomedical Optics* 17, 010901.
- Wilson, R.H., Vishwanath, K., Mycek, M.-A., 2016. Optical methods for quantitative and label-free sensing in living human tissues: Principles, techniques, and applications. *Advances in Physics*. 1–21.